IOPscience iopscience.iop.org

Home Search Collections Journals About Contact us My IOPscience

Fabrication and characterization of mesoscopic wires in GaAs

This content has been downloaded from IOPscience. Please scroll down to see the full text.

1993 Semicond. Sci. Technol. 8 2176

(http://iopscience.iop.org/0268-1242/8/12/023)

View the table of contents for this issue, or go to the journal homepage for more

Download details:

IP Address: 132.76.50.6
This content was downloaded on 17/04/2014 at 14:37

Please note that terms and conditions apply.

Semicond. Sci. Technol. 8 (1993) 2176–2183. Printed in the UK

Fabrication and characterization of mesoscopic wires in GaAs

A Ramon, M Heiblum and H Shtrikman

Submicron Semiconductor Center, Weizmann Institute of Science, Rehovot, Israel

Received 22 July 1993, accepted for publication 31 August 1993

Abstract. We report on an effort to make narrow, quasi 1D, wires in thin epilayers of n^+-GaAs, using reactive ion etching (RIE) at accelerating voltages as low as 10 V. We measure depletion widths of the order of 40 nm (while the natural width is about 20 nm). Magnetoresistance measurements on wires with electrical width of 100–300 nm show the phase coherence length of the electrons to be temperature independent below 6 K with a value close to 400 nm. At high magnetic fields (1–6 T) the magnetoresistance exhibits unusual quasi periodic oscillations, the origin of which is unclear.

1. Introduction

Reducing the dimensionality of semiconducting structures constricts the allowed phase space for charge carrier scattering, even at elevated temperatures, and thus may lead to practical devices based on electron interference. While two-dimensional structures, which are vertically structured, are the most commonly exploited to date, one- and zero-dimensional configurations need additional submicrometre lateral confinement and are thus more difficult to realize. The easiest and most common method used to reduce dimensions laterally is electrostatic confinement provided by metallic gates deposited on the surface of the two-dimensional substrate. The patterned metallic gates, however, are fragile and complicate the realization of more complex structures; there is therefore a need for a more robust confinement method. Dry (plasma) etching (the chemical or physical etching of the material by energetic ions), on the other hand, is a rugged method that precisely transfers the needed pattern and is highly anisotropic, thus enabling the creation of small structures with large aspect ratios. Unfortunately, this technique suffers from a major drawback, namely damage caused to the material by the high-energy ions hitting the surface. This damage is manifested mainly by the creation of a relatively wide region depleted of conducting carriers near the etched edges of the patterned structure. It is believed that the cause of this depletion is most likely deep electron (or hole) traps that capture the conduction band electrons (or valence band holes) [1–3].

Much work has been devoted in the past decade to studying the effects of plasma etching in GaAs. Most works have dealt with bulk n-GaAs [2, 4–6], or with heterostructures supporting a two-dimensional electron gas (2DEG) [7–12], where transport in small structures is mostly of a ballistic nature. Surprisingly, very little work has been published on the fabrication and properties of n-GaAs wires where transport is diffusive [1, 13]. In this paper we show in some detail fabrication using low-energy dry etching and the characterization of low-dimensional n-GaAs wires. We make an effort to reduce the damage by using exceedingly low-energy (10 eV) ions in the etching process. We first carry out resistance measurements in order to evaluate the depletion widths from the edges which are sensitive to the extent of the surface damage and find that they depend on the ion energy and plasma gas pressure. We find that even when we use lowest energy ions the depletion layer is twice as wide as its *natural* width from an undamaged surface. We also measure the temperature dependence of the phase coherence length, by analysis of weak localization (WL), and find it to agree with previous reported results with diffusive *one-dimensional* wires [14]. Unlike the prediction of dephasing due to electron–electron interaction (EEI), we find that the phase coherence length saturates at low temperatures. A surprising quasi periodic structure is found in the magnetoresistance at higher magnetic fields, different from the known universal conductance fluctuations (UCF). These fluctuations suggest the existence of some closed-loop trajectories, containing Aharonov–Bohm (AB) fluxes, that lead to fluctuations.

2. Sample preparation

A thin, 200 nm thick, n^+-GaAs layer, doped to 2.6×10^{18} cm^{-3}, was grown by molecular beam epitaxy (MBE), using a RIBER 2300 machine, on top of a 500 nm undoped GaAs buffer on a semi-insulating GaAs substrate. A thin etch stop layer (3 nm wide AlAs) was inserted below the n^+-GaAs layer to facilitate selectivity

0268-1242/93/122176+08 $07.50 © 1993 IOP Publishing Ltd

of etching. At 4.2 K, the measured sheet resistivity is 45 Ω $\square^{-1}$ and the mobility is 2880 $cm^2\ V^{-1}\ s^{-1}$ (as measured on large samples by standard Hall and Van der Pauw techniques), leading to a transport mean free path of some 70 nm. However, local measurements show variations (of some 20%) in these figures due to non-uniformity in the growth.

The material was patterned into narrow wires in the shape of Hall bars with different widths using electron beam lithography followed by dry plasma etching. Two basic shapes were used: *short*, where the spacing between the voltage probes is 5 or 10 times the width of the bar and bar widths vary from 0.15–1.0 μm; and *long*, with one pair of probes separated by a fixed, 35 μm long spacing, and a second pair separated by a 2 μm spacing for bar widths of 0.2–0.4 μm, and 4 μm spacing for bar widths of 0.6–1.0 μm (see inset in figure 2). The long sample is essential for suppressing the conductance fluctuations (CF) to allow a more accurate measurement of WL effects at small magnetic fields (to be shown later).

Etching is done with a customized, load-locked, ultra high vacuum (background pressure $\approx 10^{-9}$ Torr) plasma system (Nextral, NE880), operating in reactive ion etching (RIE) mode. Etching is done at two different plasma conditions, where in each set of conditions the pressure, gas flow rate and duration of the process were kept the same while the accelerating voltage varied. The process parameters are described in table 1 (processes A and B). As seen in table 1, very low accelerating voltages were used in order to minimize the damage. To preserve anisotropy, namely vertical channel walls, at the lowest accelerating voltages, gas pressure was reduced to 1 mTorr, resulting in a much reduced etching rate. For example, a rate of 90 nm min^{-1} at 5 mTorr and 35 V biasing voltage (process A) dropped to 30 nm min^{-1} at 1 mTorr (process B), necessitating longer etching times. Some representative scanning electron microscope (SEM) micrographs are shown in figure 1, illustrating the anisotropic nature of the etching process.

3. Direct resistance measurements

It is commonly found that plasma damage leads to excess depletion from the etched sides into the sample [6, 13], leading to an *electrical* width (W) smaller than the *geometrical* width (W_g). Since the cross section of the etched wire is close to being rectangular (figure 1), the resistance of the wire can be expressed as

$$R = \rho \frac{L}{W_g - d} \qquad (1)$$

where L is the wire length, W_g is the geometrical (or lithographic) width, ρ is the sheet resistance (measured in ohms), and d is the total depletion width (from both sides of the wire). Defining $g = (R/L)^{-1}$, $\sigma = \rho^{-1}$, we can rewrite equation (1) as

$$g = \sigma(W_g - d). \qquad (2)$$

Note that the free surface of GaAs is always depleted due to pinning of the Fermi level near the middle of the gap. This *natural* depletion width is given by [15]:

$$d_0 = (2\varepsilon\Phi_s/eN_D)^{1/2} \qquad (3)$$

where $\Phi_s = 0.7$ eV is approximately half the gap, $\varepsilon = 12.9\varepsilon_0$, where ε_0 is the dielectric constant of free space, and N_D is the donor concentration leading to a one-sided natural depletion width of about 20 nm in our samples.

By measuring g for different W_g, averaging it over a few wires (generally three) with the same width, and fitting the average g to a linear relation versus W_g, we obtained both σ and d from the slope of the line and its extrapolation to $g = 0$, respectively. Corrections to the non-rectangular cross section of the wires were made by viewing cleaved (long) lines with a SEM. Resistance measurements were done at 4.2 K using standard lock-in techniques are low frequencies with currents of 100 nA–1 μA, leading to voltage drops of less than 1 mV μm^{-1} (thus avoiding any heating effects).

The results show a strong dependence of the total depletion width on the accelerating voltage (see figure 2 and table 1). The values for the depletion width, quoted in table 1, are the total depletion width from both sides of the wire. We find that the depletion width created using process B (at lower pressure) is larger than the one created using process A (at similar accelerating voltages but at higher pressure), most probably due to the longer duration of that process. Similar depletion widths as in process B are also measured using ions with higher energy and higher pressure (and thus shorter etching time).

Table 1. Process parameters and depletion width. The depletion width here is the total depletion and is twice the depletion from one side.

Sample no	Process/ shape	$SiCl_4$ flow (SCCM)	Pressure (mTorr)	Etching time (min)	Cathode bias voltage (V)	Depletion width (nm)
1	A/short	25	5	3	35	83
2					50	105
3					75	110
4					100	121
5	B/long	10	1	10	11	93
6					20	131
7					35	147

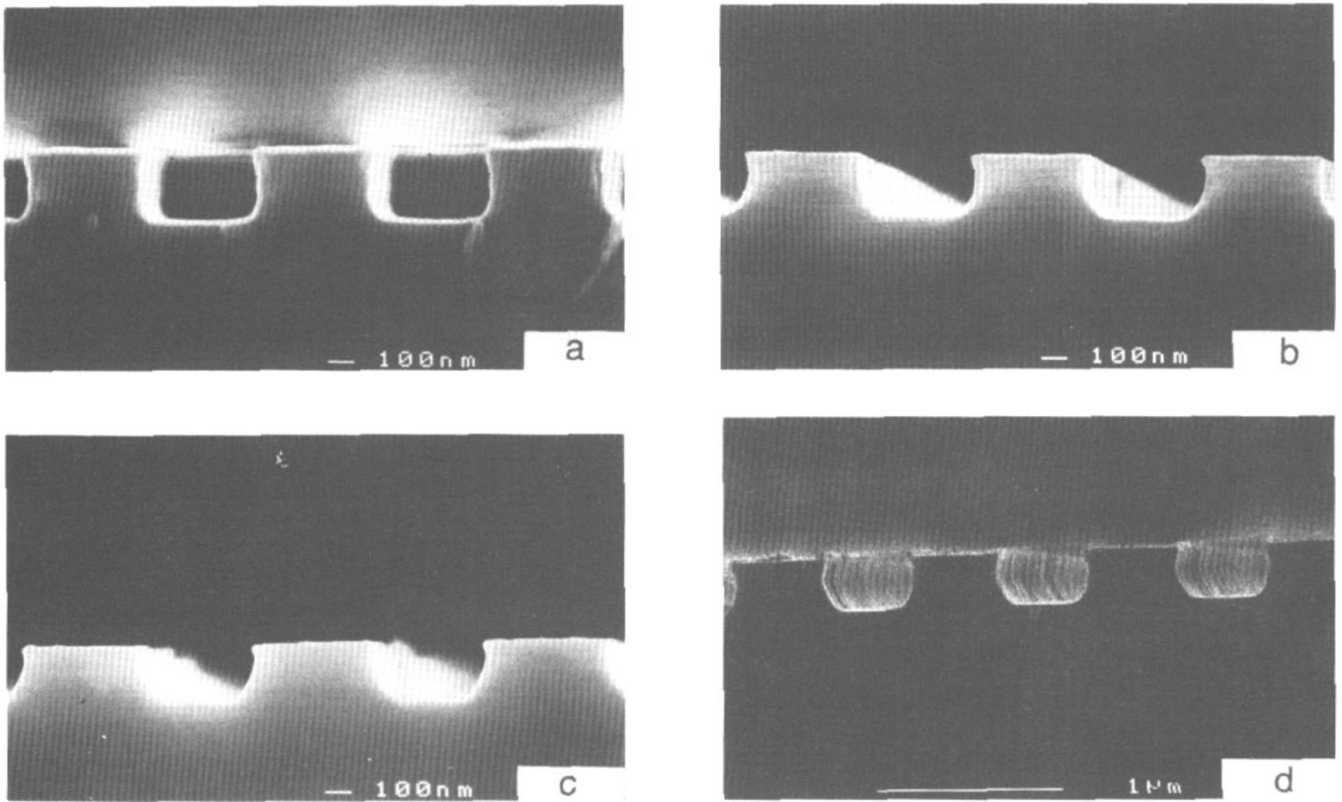

Figure 1. Cross section of narrow GaAs wires produced with $SiCl_4$ RIE processes. The gas pressure for 1 mTorr for wires (*a*) (*c*) and 5 mTorr for wire (*d*), and the bias voltages were: (*a*) 35 V; (*b*) 20 V; (*c*) 11 V; (*d*) 35 V.

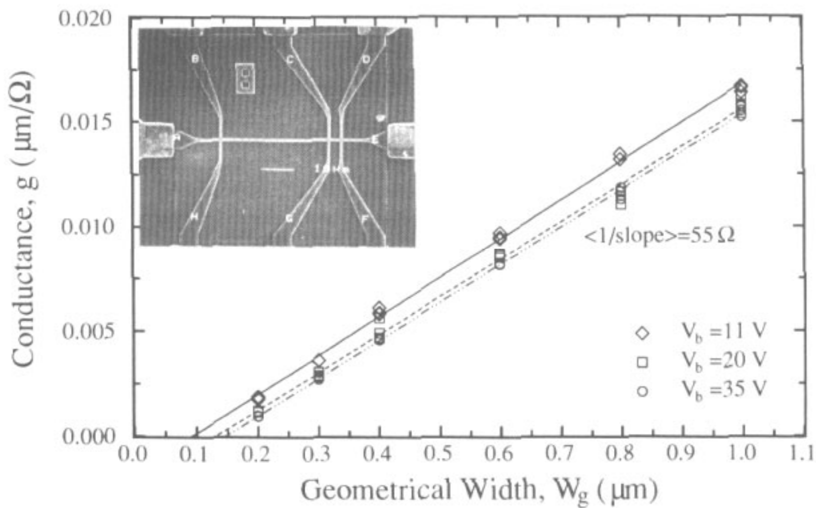

Figure 2. Dependence of the wires' conductance on the geometrical width, W_g, for different RIE bias voltages. The gas pressure for these processes was 1 mTorr. The total depletion width is the value of W_g for which the conductance is zero. The inset is a SEM micrograph of a long wire (0.8 μm width): the spacing between voltage probes B and C is 35 μm and between C and D is 4 μm; the current leads are A and E.

4. Magnetoresistance at low fields: weak localization

4.1. Theory

To characterize further the formed wires we made magnetoresistance measurements. We find characteristic negative magnetoresistance at low magnetic fields accounted for by the theory of WL. The theory of WL was first developed by Anderson *et al* [16] and Gorkov *et al* [17]. It is best understood on the basis of path integrals, in other words: the conductance of a sample depends on the electrons' probabilities of moving from a *starting* point to

an *end* point. This probability can be represented as $p_{se} = 1 - p_{bs}$, where p_{bs} is the probability to return, via backscattering, to the starting point. It is thus enough to look at p_{bs} in some detail in order to find the conductivity of the sample. The paths that return to the starting position are special: each path has its time-reversed analogue, namely, a different path that traces the original path but in the opposite direction. Because they accumulate the same phase (in the absence of magnetic field), these paths interfere constructively, thus enhancing the total probability of backscattering. In our sample the motion of the electrons is diffusive and the transport mean free path ($\approx$ 70 nm) is smaller than the sample size, leading to many interference paths and a measurable negative correction to the Drude conductivity.

Not all the possible backscattered paths contribute to an increase in the resistance: dephasing scattering events (e.g. electron–electron or electron–phonon) will randomize the electron's phase. The dephasing time, τ_ϕ, is the time needed to change the electron's phase, randomly, by the order of 2π. Obviously, time-reversed, backscattered paths that are travelled in times longer than τ_ϕ will have random phases and will not constructively interfere, thus not contributing to WL. In other words, paths that extend over distances greater than the phase coherence length, $l_\phi = \sqrt{D\tau_\phi}$, where D is the electron's diffusion constant, will not participate in the WL effect. Note that a sample of length $L \gg l_\phi$, width W and thickness t is considered to be, with respect to WL, three dimensional (3D) if both W and t are larger than l_ϕ. If both W and t, as in our case, are smaller than l_ϕ the sample is considered one dimensional (1D).

Applying a magnetic field breaks time-reversal symmetry, and identical but reversed paths will not acquire the same phase due to enclosed AB flux, leading to a suppression of WL. In this case one should consider another length scale, the magnetic length, defined as:

$$l_m \equiv (\hbar/eB)^{1/2} \tag{4}$$

where B is the magnetic field. In a magnetic field any two closed trajectories enclosing the same area S but with opposite directions will acquire an AB phase difference [18]

$$\phi = \frac{2eBS}{\hbar} \equiv \frac{2S}{l_m^2} \approx 4\pi\frac{\Phi}{\Phi_0} \tag{5}$$

where Φ is the magnetic flux through the area S and $\Phi_0 \equiv h/e$ is the elementary magnetic flux quantum. Thus, a path with area πl_m^2 will accumulate an AB phase of 2π and the negative WL correction to Drude conductivity due to this path will be lost. In a 1D wire the relevant area of the trajectories is $S \approx Wl_\phi$. Thus, in order to completely destroy WL, a field higher than $B_c \approx \pi\hbar/eWl_\phi$ is needed, where B_c is called the critical field. The exact expression [18] is

$$B_c = \frac{\hbar}{e}\frac{\sqrt{3}}{Wl_\phi}. \tag{6}$$

We can thus further refine the definition of dimensionality under the influence of magnetic field. In a wire with $W < l_\phi$, l_m the behaviour of the WL is 1D, as discussed before. For $W \approx l_m$ a crossover to 2D WL occurs since many of the trajectories that interfere constructively are those with a *diameter* smaller than l_m and hence smaller than W, making the lateral confinement less important.

For a weakly localized 1D wire, in a magnetic field B perpendicular to the wire axis, Al'tshuler *et al* [19] arrived at the following relation:

$$\frac{\Delta R}{R} \equiv \frac{R(0) - R(B)}{R(0)} = \frac{R}{L}\frac{e^2}{\pi\hbar}\left[l_\phi - \left(l_\phi^{-2} + \frac{e^2W^2B^2}{3\hbar^2}\right)^{-1/2}\right] \qquad W < l_\phi, l_m \tag{7}$$

where $R = R(0)$ is the resistance at zero magnetic field. This formula is important since it enables one to obtain the phase breaking length, l_ϕ, by simply measuring the magnetoresistance. Choi *et al* [20, 21] measured the magnetoresistance of narrow wires made with a low-mobility (2DEG). By fitting their experimental results to the above theory they were able to obtain both W and l_ϕ. Similar experiments were done with diffusive n^+-GaAs wires by Geim *et al* [14, 22] and Taylor *et al* [23], and with AlGaAs/GaAs heterostructures by Ikoma *et al* [24]. This method was also used by Wind *et al* [25] and Echternach *et al* [26] who measured the temperature dependence of the magnetoresistance of narrow and thin metal films. Since at low enough temperatures the dominant inelastic dephasing mechanism is EEI, the phase-breaking time can be approximated by the Nyquist time [27]

$$\tau_N(1D) = \left(\frac{\hbar^2 W\sigma}{e^2 k_B T\sqrt{2D}}\right)^{2/3} \tag{8}$$

while at high temperatures electron–phonon interaction becomes important and determines the phase-breaking time [25]. Echternach *et al* [26] found a good agreement with the $T^{-2/3}$ exponent, but they had a relatively large discrepancy with the prefactor (by a factor of four).

4.2. Experiments

We measured the longitudinal magnetoresistance $R \equiv R(B)$ of the fabricated wires as a function of field applied perpendicular to the wire axis and found a very clear magnetoresistance peak at zero field and quasi periodic resistance fluctuations at higher magnetic fields (to be discussed later). We show in figure 3 data for $\Delta R(B)/R(0)$, averaged over three nominally identical samples, taken at 4.2 K. The data were taken on the long samples with geometrical widths of 0.2, 0.3 and 0.4 μm using the distant spaced probes where the resistance fluctuations tend to average out to zero. The electrical width of these wires, W, as deduced from table 1, is 0.07, 0.17 and 0.27 μm, respectively, and the magnetic field, B_{1D}, defined as the field for which $l_m = W$, is 0.134, 0.023 and 0.009 T,

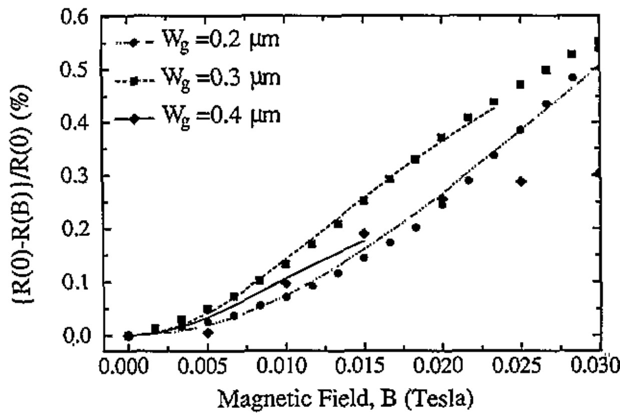

Figure 3. Magnetoresistance at different wire widths. The symbols are the experimental data and the curves are best fits of equation (7). The fits for the two wider wires stop at $B \cong B_{1D}$, while for the narrowest wire this field value falls out of the range of the graph.

respectively. Assuming that l_ϕ is larger than both the width, W, and the thickness, t, we fit the experimental data to equation (7), up to the corresponding value of B_{1D}, thus obtaining l_ϕ. We find that the coherence length changes from 0.4 to 0.33 μm as W changes from 0.07 to 0.27 μm. We note that this decrease with increasing wire width is contradictory to the expected behaviour of τ_ϕ (given in equation (8) and in [25]), governed by EEI, suggesting that at this low temperature τ_ϕ might be dominated by another scattering mechanism.

In order to check the validity of the Nyquist formula we measured the temperature dependence of the longitudinal magnetoresistance of the 0.2 μm wide wires in the temperature range 1.5–20 K, and observed a power-law behaviour in the high-temperature range followed by a saturation below 6 K (figure 4). While the theory predicts $\tau_N = 3.31 \times 10^{-11}\, T^{-2/3}$ s for our samples, the best fit to

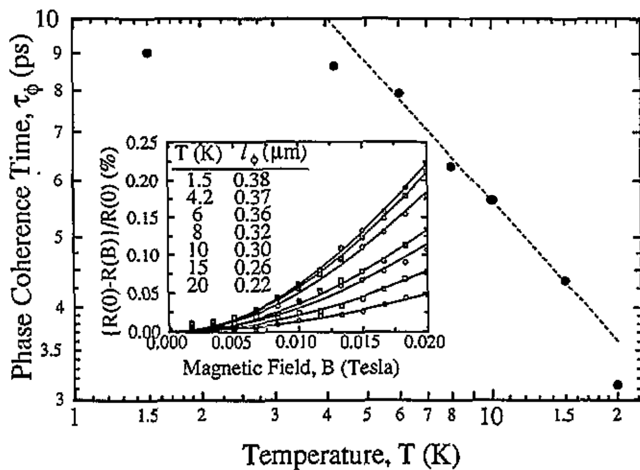

Figure 4. Phase coherence time τ_ϕ versus temperature in a wire with 0.2 μm geometrical width. The broken line is a fit to the data in the range $6 < T < 15$ K giving a slope of -0.64. For $T < 6$ K we observe saturation in τ_ϕ. In the inset we see magnetoresistance data for this wire at different temperatures and fits to equation (7) from which we obtained l_ϕ and hence τ_ϕ.

equations (7) and (8) for $6 < T < 15$ K gives $\tau_N = (2.45 \pm 0.21) \times 10^{-11} T^{-0.64 \pm 0.04}$ s, a reasonably good agreement. A similar saturation in τ_ϕ was also reported by Ikoma *et al* [24], who attributed it to random scattering from unintentional magnetic impurities.

The above discrepancy in scaling and saturation of τ_N may in our case also result from dephasing due to unintentional magnetic impurities or due to some (not understood) dephasing mechanism off the nearby edges.

5. Magnetoresistance at high fields: conductance fluctuations

5.1. Theory

As the magnetic field increases (up to 6 T) the conductance exhibits reproducible fluctuations, shown in figure 5, resembling UCF. In general, conductance fluctuations (CF) are a manifestation of the mesoscopic nature of samples small with respect to the phase-breaking length, l_ϕ. They result from different interference patterns due to the different configurations of impurities in nominally identical structures. Unlike WL, where the closed paths

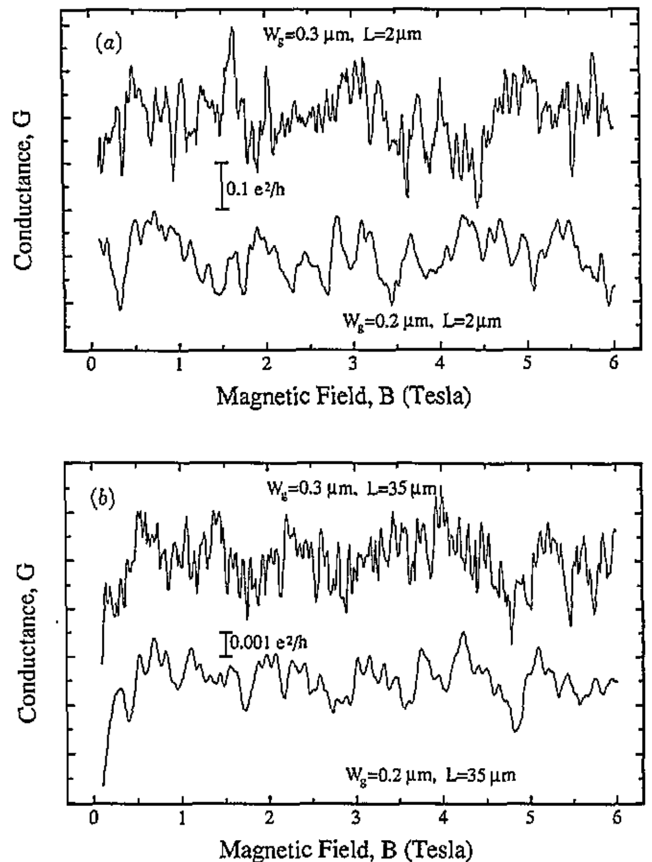

Figure 5. Conductance fluctuations as a function of magnetic field. The data were taken on long wires with geometrical widths 0.2 and 0.3 μm. The data in (*a*) were measured between the closely spaced probes and in (*b*) between the distantly spaced probes. The resistance of the 0.2 μm wire is about 1.4 (30) kΩ for the close (distant) configuration and is about 0.6 (12) kΩ for the close (distant) configuration of the 0.3 μm wire.

play a dominant role, in CF the interference of the forward-scattered paths is important. The Al'tshuler-Lee-Stone theory of UCF [28, 29] predicts a universal RMS value for these CF, $\delta G \approx e^2/h$ at $T = 0$, when phase coherence is maintained over the whole sample. Since in practice these sample-to-sample fluctuations are hard to measure, they are generally studied in a single sample as a function of a changing magnetic field that changes the phases of the electrons' wavefunctions. These two methods are equivalent, and this 'ergodic hypothesis' is proved in [30].

As the temperature is raised above zero the size of the fluctuations decreases below e^2/h owing to a reduction in l_ϕ and to thermal averaging. A long wire, with $W \ll l_\phi \ll L$, can be divided into L/l_ϕ short segments, each segment having fluctuations of the order of e^2/h. Neglecting thermal smearing, the size of the CF of a long wire is of the order of [31]

$$\delta G = \text{constant} \times \frac{e^2}{h}\left(\frac{l_\phi}{L}\right)^{3/2}. \qquad (9)$$

At $T = 0$ all interfering electrons have the same energy and all accumulate the same phase if they traverse the same path in the material. However, at $T > 0$, electrons are energetically spread over an interval of $k_B T$ and accumulate phase differences among themselves, even if they traverse similar paths. In a time interval t, two electrons with an energy difference δE will accumulate a phase difference $\delta\varphi \approx t\delta E/\hbar$ and travel a distance $L = (Dt)^{1/2} \approx (\hbar D/\delta E)^{1/2}$ to acquire $\delta\varphi$ of the order of unity. The thermal length, L_T, is defined such that $\delta E \equiv k_B T$, that is

$$L_T = (\hbar D/k_B T)^{1/2} \qquad (10)$$

is the length electrons travel in order to accumulate a phase difference among themselves of order unity. The effect of thermal smearing is important only when $l_\phi \gg L_T$. In this case we can divide the energy interval $k_B T$ into N subintervals of magnitude $\delta E(l_\phi)$ with $N = k_B T/\delta E(l_\phi) = (l_\phi/L_T)^2$. Assuming that these intervals are uncorrelated the RMS variation of the conductance, δG will be reduced by a factor $N^{-1/2} \approx L_T/l_\phi$ with respect to equation (9) [31, 32]

$$\delta G = \text{constant} \times \frac{e^2}{h}\frac{L_T l_\phi^{1/2}}{L^{3/2}} \qquad \text{if } l_\phi \gg L_T. \quad (11)$$

Beenakker and Van Houten [33] have evaluated the unspecified constant which appears in equations (9) and (11) and have given an interpolation formula that also holds for the intermediate regime $l_\phi \approx L_T$:

$$\delta G = \sqrt{6}\,\frac{e^2}{h}\left(\frac{l_\phi}{L}\right)^{3/2}\left[1 + \frac{9}{2\pi}\left(\frac{l_\phi}{L_T}\right)^2\right]^{-1/2} \qquad (12)$$

where the prefactor is appropriate for our GaAs sample and a magnetic field higher than B_c (equation (6)). The equivalence between sample-to-sample CF and single-sample magnetoconductance fluctuations derives from the fact that the conductance at a field B is uncorrelated with that at $B + \Delta B$, when ΔB is larger than a correlation field ΔB_{cor} [28]. Generally, the correlation field is small enough not to modify the statistical properties of the ensemble. The correlation function is given by:

$$F(\Delta B) \equiv \langle [G(B) - \langle G(B)\rangle] \times [G(B + \Delta B) - \langle G(B + \Delta B)\rangle]\rangle \qquad (13)$$

where the angle brackets denote averaging over B. Note that δG is just $F(0)^{1/2}$. The correlation field ΔB_{cor} is defined from the correlation function $F(\Delta B_{cor}) \equiv F(0)/2$, and is [31]

$$\Delta B_{cor} = 2\pi C \frac{\hbar}{e}\frac{1}{W l_\phi} \qquad (14)$$

where the prefactor $C(l_\phi, L_T)$ decreases from 0.95 for $l_\phi \gg L_T$ to 0.42 for $l_\phi \ll L_T$ [33].

5.2. Experiments

Typical data for $R(B)$ taken on the long samples, measured between the closely spaced probes (2 μm) and the distantly spaced probes (35 μm), are shown in figure 5. As is clearly evident the fluctuations are much smaller in the distantly spaced configuration (note the different vertical scales). Averaging δG and ΔB_c for three nominally identical wires we obtain for $W_g = 0.2$ μm, $\delta G = 2.25 \times 10^{-6}$ (3.84×10^{-8}) Ω^{-1} for the close (distant) configuration and for $W_g = 0.3$ μm, $\delta G = 2.45 \times 10^{-6}$ (4.66×10^{-8}) Ω^{-1} for the close (distant) configuration. Using $D = 0.016$ m^2 s^{-1}, $L_T = 0.17$ μm (at 4.2 K) and the value of l_ϕ obtained from WL, the results for δG agree with equation (12) to within 20%. Also $\delta G(35\ \mu\text{m})/\delta G(2\ \mu\text{m}) = 0.018$ whilst the theoretical value is $(2/35)^{3/2} = 0.014$.

In order to independently estimate l_ϕ the correlation function was calculated and plotted in figure 6. We find $\Delta B_{cor} = 0.092$ (0.100) T for the close (distant) configuration in the 0.2 μm wires and $\Delta B_{cor} = 0.039$ (0.041) T for the close (distant) configuration in the 0.3 μm wires. The ratio between the correlation fields of the different widths agrees well with the expected ratio (the inverse ratio of

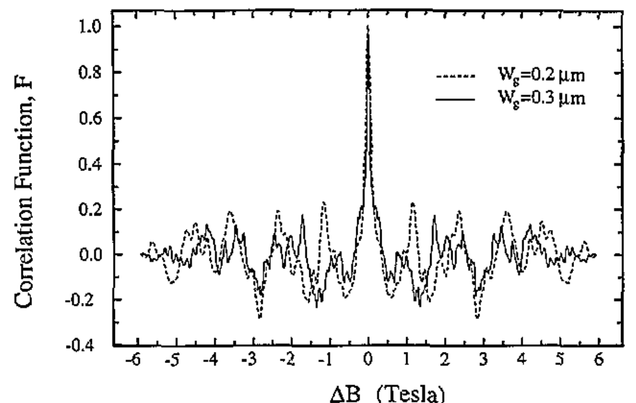

Figure 6. Normalized correlation function of the conductance fluctuations of figure 5(a). The correlation field, ΔB_{cor}, is about 0.09 T in the narrow wire and about 0.04 in the wide wire. Note the oscillating tail of the correlation function.

electrical widths). The value for l_ϕ obtained from equation (14) for all widths and probe spacings agrees well with the value obtained from WL if we take the unspecified constant in equation (14) to be about 0.65 (in agreement with the fact that $l_\phi \approx L_T$).

Unexpectedly, the correlation function (figure 6) does not vanish for fields greater than the correlation field but keeps fluctuating, suggesting correlation in the fluctuations, or in other words, some periodic fluctuations. To check that hypothesis we performed a direct Fourier transform of the fluctuations, in order to obtain their spectra, and observed rather distinct frequencies (in B^{-1}), with a most distinct frequency around 0.5-1 T^{-1} (seen in figure 7). This corresponds to an approximated area formed by two scattering events separated by the transport mean free path of our samples ($\approx$ 70 nm). An explanation offered by Taylor *et al* [23] makes use of this fact.

Among all possible closed trajectories responsible for WL there are few in which the electron goes through a very small (say less than 10) number of scattering events. The resistance then oscillates due to the change in AB flux through these trajectories with frequencies $f = (2e/h)S$ (see equation (5)), where S is the area of each trajectory. As in WL, the amplitude of the resistance oscillations should be proportional to $\exp(-2l/l_\phi)$, where l is the path length and the factor 2 accounts for the total path length accumulated by the opposite trajectories. However, unlike in WL, where the many different frequencies (due to the large number of trajectories) average out to zero for $B > B_c$, the total averaged amplitude here is finite. For small trajectories, with a small number of scattering events, the path length, l, is related to the area, S, via $l = \alpha S^{1/2}$ where, as examples, $\alpha = 4.5$ for an equilateral triangle and $\alpha = 3.5$ for a circular trajectory. Thus, if we have a certain number of very similar trajectories (with similar α), the amplitude of their WL-related CF is

$$a(f) \propto \exp\left[-2\alpha\left(\frac{h}{2e}\right)^{1/2} f^{1/2} l_\phi^{-1}\right]. \qquad (15)$$

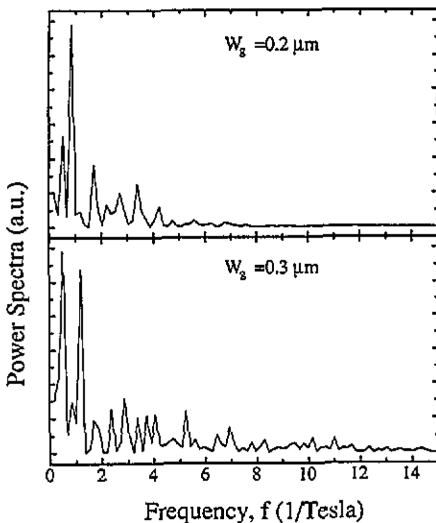

Figure 7. Fourier power spectra of the conductance fluctuations of figure 5(a).

In figure 8 we plot the logarithmic dependence of the data presented in figure 7 versus the square root of the frequency ($B^{-1/2}$). From the slope of the full line, approximating the average of the data points and the known value for l_ϕ, we extract the constant α. We obtain $\alpha \approx 4.6$ for $W = 0.07$ μm wires and $\alpha \approx 2.8$ for $W = 0.17$ μm wires (an unphysically small value for α). Even though the experimental agreement with this model seems correct at first sight, it is difficult to picture how it could be realized in practice with all possible trajectories. For example, the presence of higher frequencies suggests larger trajectories, *but with the same* α, namely, trajectories that could not be fitted into our quasi 1D wires. Note also that the 2D regions where the ohmic contacts are formed are separated by more than l_ϕ from the quasi 1D channels (see the inset in figure 2) and thus trajectories that *wander* there are totally dephased. Thus, we believe that this explanation is questionable at the present.

Another possibility, which, however, does not give the same spectral dependence, is that the fluctuations can originate from AB fluxes threading some insulating defects 60 nm and more in size. However, we find no reason for our n-GaAs samples to have these defects (they could be accounted for by depletion regions surrounding dislocations, but the dislocation density in our samples is $< 10^4$ cm^{-2}, much too small to be observed).

6. Conclusions

We have described in some detail the fabrication and characterization of low-dimensional n-GaAs wires, 0.15–1 μm wide. Fabrication was done with a low energy (as low as 10 eV) reactive ion etching process, and demonstrated the feasibility of anisotropic etching. We find that the width of the depletion layer from the edges of the wires is strongly dependent on process parameters but is always larger than the natural depletion distance. This disap-

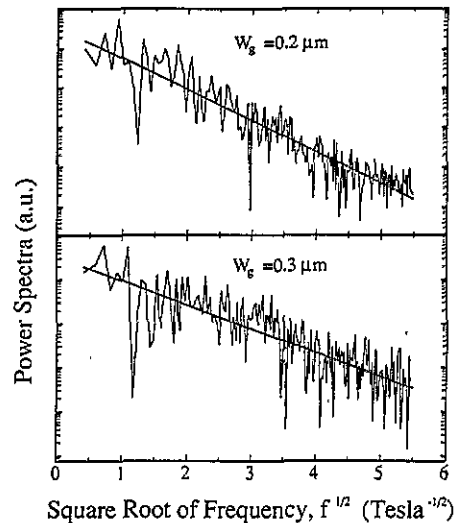

Figure 8. The same Fourier power spectra as in figure 7 plotted on a logarithmic scale versus the square root of the frequency. The straight lines are fits giving $\alpha \approx 4.6$ for the narrow wire and $\alpha \approx 2.8$ for the wide wire.

pointing result is probably due to the low etching rate and the consequently long etching times of the process.

We measured the low-temperature magnetoresistance of these wires and obtained (via the analysis of weak localization and the universal conductance fluctuations) the phase-breaking length and its temperature dependence, and find it to be governed by electron–electron interactions at temperatures above 6 K. At lower temperatures the phase coherence length saturates at about 400 nm, most probably due to scattering from magnetic impurities. Surprisingly, the conductance fluctuations at magnetic fields higher than 1 T exhibit a quasi periodic structure, suggesting Aharonov–Bohm interference through some closed loops. These loops could originate from small insulating regions in the structure (of unclear origin) or from small closed trajectories that contribute to the non-zero net resistance fluctuations.

Acknowledgments

We wish to thank A G Aronov and C Beenakker for useful discussions and U Meirav, D E Prober, I Bar Joseph and A Yacoby for constructive suggestions. The work was partly supported by the Israeli Defense Ministry, grant no 131262-593-1390-8-102.

References

[1] Rahman M, Johnson N P, Foad M A, Long A R, Holland M C and Wilkinson C D W 1992 *Appl. Phys. Lett.* **61** 2335
[2] Seaward K L, Moll N J and Stickle W F 1990 *J. Electron. Mater.* **19** 385
[3] Seaward K L and Moll N J 1992 *J. Vac. Sci. Technol.* B **10** 46
[4] Lootens D, Van Daele P, Demeester P and Clauws P 1991 *J. Appl. Phys.* **70** 221
[5] Cheung R, Thoms S, Watt M, Foad M A, Sotomayor-Torres C M, Wilkinson C D W, Cox U J, Cowley R A, Dunscombe C and Williams R H 1992 *Semicond. Sci. Technol.* **7** 1189
[6] Foad M A, Thoms S and Wilkinson C D W 1993 *J. Vac. Sci. Technol.* B **11** 20
[7] Knoedler C M, Osterling L and Shtrikman H 1988 *J. Vac. Sci. Technol.* B **6** 1573
[8] Knoedler C M, Osterling L and Heiblum M 1989 *J. Appl. Phys.* **65** 1800
[9] Swaminathan V, Asom M T, Chakrabarti U K and Pearton S J 1991 *Appl. Phys. Lett.* **58** 1256
[10] Germann R, Forchel A, Bresch M and Meier H P 1989 *J. Vac. Sci. Technol.* B **7** 1475
[11] Beinstingl W, Christanell R, Smoliner J, Wirner C, Gornik E, Weimann G and Schlapp W 1990 *Appl. Phys. Lett.* **57** 177
[12] Skidmore J A, Green D L, Young D B, Olsen J A, Hu E L, Coldren L A and Petroff P M 1991 *J. Vac. Sci. Technol.* B **9** 3516
[13] Long A R, Rahman M, MacDonald I K, Kinsler M, Beaumont S P, Wilkinson C D and Stanley C R 1993 *Semicond. Sci. Technol.* **8** 39
[14] Geim A K, Main P C, Beton P H, Streda P, Eaves L, Wilkinson C D W and Beaumont S P 1991 *Phys. Rev. Lett.* **67** 3014
[15] Sze S M 1969 *Physics of Semiconductor Devices* (New York: Wiley-Interscience)
[16] Anderson P W, Abrahams E and Ramakrishnan T V 1979 *Phys. Rev. Lett* **43** 718
[17] Gorkov L P, Larkin A I and Khemel'nitskii D E 1979 *Pisma Zh. Eksp. Teor. Fiz.* **30** 248 (Engl. transl. 1979 *JETP Lett.* **30** 228)
[18] Beenakker C W J and Van Houten H 1991 *Solid State Physics* vol 44 ed H Ehrenreich and D Turnbull (San Diego, CA: Academic)
[19] Al'tshuler B L and Aronov A G 1981 *Pisma Zh. Eksp. Teor. Fiz.* **33** 515 (Engl. transl. 1981 *JETP Lett.* **33** 499)
[20] Choi K K, Tsui D C and Alavi K 1987 *Appl. Phys. Lett.* **50** 110
[21] Choi K K, Tsui D C and Alavi K 1987 *Phys. Rev.* B **36** 7751
[22] Geim A K, Main P C, Beton P H, Eaves L, Beaumont S P and Wilkinson C D W 1992 *Phys. Rev. Lett.* **69** 1248
[23] Taylor R P, Leadbeater M L, Whittington G P, Main P C, Eaves L, Beaumont S P, McIntyre I, Thoms S and Wilkinson C D W 1988 *Surf. Sci.* **196** 53
[24] Ikoma T, Odagiri T and Hirakawa K 1992 *Quantum Effect Physics, Electronics and Applications (Inst. Phys. Conf. Ser. 127)* ed K Ismail *et al* (Bristol: IOP Publishing) p 157
[25] Wind S, Rooks M J, Chandrasekhar V and Prober D E 1986 *Phys. Rev. Lett.* **57** 633
[26] Echternach P M, Gershenson M E, Bozler H M, Bogdanov A L and Nilson B unpublished
[27] Al'tshuler B L, Aronov A G and Khmelnitskii D E 1982 *J. Phys. C: Solid State Phys.* **15** 7367
[28] Al'tshuler B L 1985 *Pis'ma Zh. Eskp. Teor. Fiz.* **41** 530 (Engl. transl. 1985 *JETP Lett.* **41** 648)
[29] Lee P A and Stone A D 1985 *Phys. Rev. Lett.* **55** 1622
[30] Al'tshuler B L, Kravtsov V E and Lerner I V 1986 *Pis'ma Zh. Eksp. Teor. Fiz.* **43** 342 (Engl. transl. 1986 *JETP Lett.* **43** 441)
[31] Lee P A, Stone A D and Fukuyama H 1987 *Phys. Rev.* B **35** 1039
[32] Al'tshuler B L and Khmel'nitskii D E 1985 *Pis'ma Zh. Eskp. Teor. Fiz.* **42** 291 (Engl. transl. 1985 *JETP Lett.* **42** 359)
[33] Beenakker C W J and Van Houten H 1988 *Phys. Rev.* B **37** 6544